Development of reflective back contacts for high-efficiency ultrathin $Cu(In,Ga)Se_2$ solar cells

Louis Gouillart[1,3,*], Andrea Cattoni[1], Julie Goffard[1], Frederique Donsanti[2], Gilles Patriarche[1], Marie Jubault[2], Negar Naghavi[3], Stéphane Collin[1]

[1] Centre for Nanoscience and Nanotechnology (C2N), CNRS, Univ. Paris-Sud, Université Paris-Saclay, 91120 Palaiseau, France

[2] EDF R&D, IPVF, 30 Route Départementale 128, 91120 Palaiseau, France

[3] CNRS, UMR 9006, IPVF, 30 Route Départementale 128, 91120 Palaiseau, France

*corresponding author at: Centre for Nanoscience and Nanotechnology (C2N/CNRS), 91120 Palaiseau, France. E-mail address: *louis.gouillart@c2n.upsaclay.fr* (L. Gouillart)

Abstract

Because of poor light absorption, $Cu(In,Ga)Se_2$-based (CIGS) solar cells with an ultrathin absorber layer (<500 nm) require the development of reflective back contacts. To enhance rear reflectance in CIGS ultrathin devices, we investigate novel back contact architectures based on a silver metallic mirror covered with a thin layer of In_2O_3:Sn (ITO), which is fully compatible with nanopatterning for further light trapping improvements. First, numerical electromagnetic simulations of complete solar cells have been performed for a 490 nm thick CIGS absorber with various back contacts. We predict a short-circuit current density of J_{SC} = 34.0 mA/cm^2 for a 490 nm thick CIGS absorber with a silver nanostructured mirror. Second, we have fabricated and characterized 490 nm thick CIGS solar cells with transparent back contacts made of ITO, and reflective back contacts made of silver covered with ITO. Solar cells with a transparent ITO back contact exhibit an average efficiency of 10.0 %, compared to 9.3 % for standard molybdenum back contacts. A 5 nm thick Ga_2O_3 layer is revealed at the ITO/CIGS interface by transmission electron microscopy and energy dispersive X-ray spectroscopy. When silver is added, the reflective back mirror leads to a J_{SC} improvement of 4.6 mA/cm^2 (from 22.4 to 27.0 mA/cm^2). These results pave the way for efficient ultrathin CIGS solar cells on reflective back contacts.

Keywords

Solar cells, Copper indium gallium selenide, Ultrathin films, Transparent back contact, Reflective back contact, Nanostructured back mirror

1. Introduction

$Cu(In,Ga)Se_2$-based (CIGS) solar cells are one of the most promising thin-film technologies, with a record efficiency of 22.9 % achieved with a 2–3 µm thick absorber [1], [2]. However, the scarcity and high cost of Indium are a drawback for industrial production of competitive modules. With a CIGS absorber thickness lower than 500 nm it is possible to reduce deposition time and materials consumption, resulting in a decreased manufacturing cost [3], [4].

Ultrathin CIGS-based solar cells exhibit lower short-circuit current densities (J_{SC}) and efficiencies mainly due to lower light absorption, enhanced recombination [5] and low reflectivity of the conventional Mo back contact [6], [7]. These loss mechanisms can be overcome by substituting the Mo back contact with passivating and more reflective back contact. Up to now, there are few studies of reflective back contacts for CIGS solar cells, such as: direct use of reflective or metallic back contacts [8]–[10], a combination of transparent conducting oxide and metallic reflector [7], passivating reflective back contact [11], or nanostructured back contacts [12], [13]. Nanostructured back reflectors are a promising strategy for enhanced absorption in ultrathin CIGS layers, as they lead to calculated J_{SC} up to 36.3 mA/cm^2 in a 150 nm thick CIGS layer compared to 23.5 mA/cm^2 with a standard Mo back contact [12]. Nanostructured mirrors have also yielded significant J_{SC} improvements in other types of solar cells such as amorphous Si:H [14] and ultrathin GaAs [15], [16].

In this paper we present the first steps towards the development of a reflective back contact based on a silver metallic mirror encapsulated with a thin layer of In_2O_3:Sn (ITO). Reflective back contacts for CIGS solar cells need not only to provide enhanced rear reflectance but also to form an ohmic contact with the absorber. Several studies report on the formation of a resistive interfacial layer of Ga_2O_3 after CIGS deposition on oxide layers such as hydrogen-doped In_2O_3, ITO, MoO_3, SnO_2:F, ZnO or ZnO:Al [17]–[22]. In particular, ITO is known to prevent Na diffusion from the glass to the CIGS absorber and to form a detrimental layer of Ga_2O_3 for CIGS deposition temperatures above 520 °C [22], [23]. As a result, the stability and electrical properties of ultrathin devices on transparent ITO-based substrates were first investigated by co-evaporation of CIGS at low temperature (450°C) with incorporation of Na from a NaF post-deposition treatment.

In this study, the improvement of light absorption in a 490 nm thick CIGS absorber is first simulated using a nanostructured and a flat mirror encapsulated in transparent conducting oxides such as ITO. Then, the optical properties of glass substrates covered with Mo, Ag and Ag/ITO are determined and compared. 490 nm thick CIGS solar cells are fabricated on ITO back contacts, and the ITO/CIGS interface is studied in-depth with transmission electron microscopy (TEM) and energy dispersive X-ray spectroscopy (EDX). The performances of cells on ITO and Mo back contacts are compared and discussed, and preliminary results on Ag/ITO back contacts are presented.

2. Experimental methods

CIGS solar cells were fabricated on soda-lime glass (SLG) substrates with three different back contacts. The first stack is made of a conventional 800 nm thick molybdenum (Mo) back contact deposited on a 300 nm Al_2O_3 layer that acts as a diffusion barrier for alkali elements present in SLG. Al_2O_3 is deposited by atomic layer deposition. The second stack is based on a transparent 300 nm thick ITO layer sputtered on SLG. The third stack contains a 30 nm thick ITO sputtered on a 150 nm thick Ag layer deposited by electron beam evaporation. A 490 nm thick CIGS layer was deposited by thermal co-evaporation in a one-stage process, at a fixed substrate temperature of 450 °C. This substrate temperature was calibrated in a previous work, using an infrared camera [24]. Average composition of absorbers was determined from X-Ray Fluorescence (XRF) signal of CIGS deposited on Mo, leading to atomic ratios of [Cu]/([In]+[Ga]) = 0.81 ± 0.01 (CGI) and [Ga]/([Ga]+[In]) = 0.32 ± 0.01 (GGI). A NaF post-deposition treatment was applied with an evaporation rate of 1 nm/min under Se flux and at fixed substrate temperature of 350 °C. Solar cells were completed with the standard front layer stack consisting in a chemical bath deposited CdS/rf-sputtered ZnO/rf-sputtered ZnO:Al with respective thicknesses 50nm/50nm/400nm determined by XRF analysis on control samples.

Opto-electrical properties of ITO were determined from a 200 nm thick ITO layer sputtered on SLG. As annealing of ITO improves its optical transparency and carrier mobility, its optical indices and resistivity were measured before and after a 10-minute-annealing performed in air on a hotplate set at 540 °C. Refractive index n and extinction coefficient k were extracted from ellipsometric measurements on a UVISEL ellipsometer from Horiba Jobin-Yvon. The ITO resistivity was measured with a four-point probe system before (ρ = $9.0x10^{-4}$ Ω.cm) and after annealing (ρ = $7.0x10^{-4}$ Ω.cm). Finally, a Sentech reflectometer was used to determine the spectral reflectance of four different substrates: SLG/600-nm-Mo, SLG/150-nm-Ag, SLG/150-nm-Ag/30-nm-ITO and SLG/150-nm-Ag/200-nm-ITO substrates.

Current-voltage I(V) measurements of 0.1 cm^2 solar cells were carried out with a Newport class AAA solar simulator under AM1.5G illumination and in the dark. Devices on transparent substrates were placed on a black paper before light I(V) measurements to avoid additional rear-reflection from the substrate holder. External Quantum Efficiency (EQE) measurements were performed with a IQE200 Newport Instrument. A slab of a 490 nm thick CIGS layer deposited on an ITO-based transparent back contact was prepared by a focused ion beam, and analysed with TEM in a FEI Titan Themis XFEG instrument at an acceleration voltage of 200 kV. Composition mappings were determined by EDX.

3. Results and discussion

3.1 Absorption simulation

We first investigate numerically the optical effects of a nanostructured back mirror, a flat back mirror, and a transparent back contact as compared to a conventional Mo back contact. The spectral absorption is simulated with a rigorous coupled wave analysis method, and the optical indices are calculated from ellipsometric measurements for CIGS and annealed ITO, and taken from the literature for other materials. More details can be found in reference [12]. The architecture of flat ultrathin devices is sketched in Fig. 1a), while the optimized geometry of a complete device including a nanostructured back mirror is presented in Fig. 1b) and c). This simulated nanostructured back mirror consists of square-shaped dielectric nanogrid on top of a flat ITO-coated Ag stack. The dielectric nanogrid has a refractive index of $n = 1.5$, a height of 200 nm, a period of 600 nm and hole width of 350 nm. The experimental fabrication of such a dielectric nanogrid is under development, using a scalable process based on direct nanoimprint of a sol-gel derived metal oxide [25], [26]. The simulated absorptions of CIGS devices on Mo, ITO, as well as flat and nanostructured reflective back contacts are plotted in Fig. 2.

As shown in Fig. 2a, using a standard Mo back contact leads to substantial absorption losses for long wavelengths (> 600 nm), because of the low reflectivity at CIGS/Mo interface. Moreover, optical losses are also observed at short wavelengths (< 500 nm) due to the low bandgap of CdS (2.4 eV) buffer layer. Assuming a perfect collection of photogenerated carriers, a theoretical short-circuit current density J_{SC} can be deduced from the simulated CIGS absorption [12]. It is limited to 28.8 mA/cm^2 with a Mo back contact. When Mo is replaced by ITO (Fig. 2b) a similar spectral absorption with a J_{SC} of 28.5 mA/cm^2 is calculated. The introduction of an Ag layer results in enhanced back reflectance and significant improvement of CIGS light absorption at long wavelengths (> 800 nm), (Fig. 2c), which leads to an increased J_{SC} of 32.2 mA/cm^2. Finally, if the flat mirror is replaced by an optimised nanostructured back mirror made of a nanogrid, additional absorption resonances occur close to the bandgap (Fig. 2d). Multi-resonant absorption in the thin CIGS layer leads to a J_{SC} of 34.0 mA/cm^2, which represents an additional 1.8 mA/cm^2 gain as compared to the flat back mirror.

3.2 Optical characterization of back contacts

Before deposition of CIGS on transparent and reflective back contacts, the spectral reflectance of 4 different back contacts deposited on SLG were first measured and compared: a 600 nm thick Mo, a 150 nm thick Ag layer, and 150 nm thick Ag layers with 30 nm and 200 nm ITO coatings (Fig. 3a). As expected, Mo has a low reflectivity and cannot act as a back mirror, resulting in low CIGS absorption for ultrathin CIGS solar cells (Fig. 2a). On the contrary, the silver layer provides a high reflectivity (R>90 % for λ>500 nm), but it cannot be used as a back contact due to diffusion of Ag in CIGS during the growth. When the silver layer is covered with ITO coatings, the reflectivity is significantly reduced due to parasitic absorption. Reflectivity dips are attributed to Fabry-Perot resonances in the ITO layer. After a 10-minute-annealing in air at 540 °C, the reflectivity is strongly enhanced and exceeds 90 % for wavelengths above 550 nm. This annealing experiment performed in air proves that the ITO layer efficiently encapsulates the Ag mirror, preventing its oxidation and morphological changes that negatively impact its reflectivity; the stability of such reflective back contact under CIGS deposition was only tested after the complete solar cell fabrication. To determine the origin of the enhanced reflectivity of Ag/ITO stacks after annealing, ellipsometric measurements were carried out on a 200 nm thick ITO layer sputtered on SLG before and after annealing in air at 540 °C during 10 minutes. The refractive index n and extinction coefficient k are displayed in Fig. 3b). The annealing results in an increase of n and a decrease of k in the visible and infrared domains (λ>500 nm). The origin of these effects was not investigated in detail, though it is commonly accepted that annealing of amorphous ITO generally results in an increased layer density, an improved carrier mobility and a reduced free-carrier absorption. It leads to a significant improvement of the Ag/ITO reflectivity and a spectral shift of the reflectivity dips toward shorter wavelengths (Fig. 3a).

3.3 TEM-EDX back contact characterization

A TEM-EDX analysis was performed in order to investigate the ITO/CIGS interface. Fig. 4a) and b) show a TEM image of an ultrathin 490-nm-CIGS layer deposited on an ITO back contact along with the average composition profile of absorber elements deduced from EDX analysis. An average GGI of 0.28 was calculated from the average EDX signal of the CIGS layer, which is close to the GGI value of 0.32 determined by XRF. It is worth mentioning that the EDX signal of Cu is overestimated as Cu from the substrate holder is also detected. Hence CGI cannot be deduced from this analysis.

This EDX analysis confirms that the CIGS composition is homogeneous from the front to the back interface, as expected from a one-stage CIGS deposition process. Moreover it reveals that Ga segregates at the back contact.

Closer views are shown in Fig. 4. with (c) an additional dark field TEM image and its corresponding compositional EDX mappings of O, Ga, In, and Se elements. They reveal a segregation of both Ga and O elements at the ITO/CIGS interface, which suggests that a thin Ga_2O_3 layer is formed during CIGS deposition. This layer should be highly resistive and possibly n-doped [17]. However, in this study the low substrate temperature (450 °C) during CIGS deposition results in a very thin Ga_2O_3 layer of only 5 nm that does not seem to deteriorate solar cell performances.

3.4 Solar cell performances

The performances of ultrathin CIGS solar cells are summarized in Table 1 for Mo and ITO back contacts. Best efficiencies are given together with average I(V) parameters and standard deviation for the 10 best cells. Dark I(V) parameters are extracted from the fit of a 2-diode model: saturation currents for diodes with ideality factors of 1 (J_{01}) and 2 (J_{02}), shunt resistance (R_{SH}) and series resistance (R_S). I(V) and EQE curves of best cells are displayed on Fig. 5, together with the experimental EQE of a 490 nm thick CIGS cell on a reflective back contact (Ag). The reference solar cells on a SLG/Al_2O_3/Mo substrate exhibit an average efficiency of 9.3 %.

Ultrathin CIGS solar cells with an ITO back contact present an average efficiency of 10.0 %. Mo and ITO-based substrates lead to very close dark currents (J_{01}, J_{02}), R_{SH} and fill factors (FF). A slight increase of R_S is observed with an ITO back contact, from 0.1 for Mo to 1.2 $\Omega.cm^2$. Importantly, the increase of both open-circuit voltage and J_{SC} results in an absolute efficiency enhancement of 0.7 %. It indicates that ITO has suitable electrical properties to be used as a back contact in CIGS solar cells. Ultrathin CIGS devices on transparent SLG/ITO substrates could be used for bifacial solar cells. Alternatively, solar cell efficiency could be enhanced by adding a mirror on the backside of the glass substrate.

According to simulation results (Fig. 2), the short-circuit current could also be increased by adding a flat silver back mirror between the ITO layer and the glass substrate, with an expected gain of 4.6 mA/cm^2 over the Mo reference. We have performed preliminary experiments of 490 nm thick CIGS solar cells deposited on reflective multilayer stacks (MLS) based on silver covered by ITO. They led to poor electrical performances due to process issues that should be overcome by further optimizations. However, the reflective MLS resulted in a strong EQE enhancement. The EQE of ultrathin solar cells with a Mo back contact, an ITO back contact, and a reflective MLS are plotted and compared in Fig. 5b. The reflective back contact leads to an improvement for wavelengths above 500 nm and results in a promising J_{SC} = 27.0 mA/cm^2. The same EQE measurements are also plotted and compared to numerical simulation in Fig. 2. A very good agreement between experiments and simulations is obtained.

5. Conclusion

Ultrathin CIGS solar cells with transparent and reflective back contacts were first numerically investigated. A J_{SC} of 32.2 mA/cm^2 is calculated for 490 nm thick CIGS solar cells with a flat back mirror, corresponding to a 3.4 mA/cm^2 gain as compared to standard molybdenum back contacts. An additional optical gain is predicted with a nanostructured reflective back contact, leading to a J_{SC} of 34.0 mA/cm^2. Flat reflective stacks of Ag/ITO were fabricated and are stable under a 10-minute-annealing in air at 540 °C. Their spectral reflectance is over 90 % for wavelengths above 550 nm, which should substantially increase absorption in ultrathin CIGS absorbers. Complete ultrathin CIGS solar cells were fabricated on molybdenum and transparent ITO back contacts, with respective average efficiencies of 9.3 % and 10.0 %. ITO forms an ohmic back contact with CIGS, as confirmed by an average FF of 70.3 %. A TEM-EDX investigation shows that the thickness of the Ga_2O_3 formed at ITO/CIGS interface during CIGS deposition is limited to 5 nm and has no impact on solar cell performances. Preliminary experiments on reflective back contacts made of Ag and ITO led to a J_{SC} = 27.0 mA/cm^2. These results provide a promising route toward efficient, ultrathin CIGS solar cells deposited on reflective back contacts.

Acknowledgements

This work is supported by the ARCIGS-M project within the European Union's Horizon 2020 research and innovation program under grant agreement No. 720887.

References

[1] "Solar Frontier press release dated December 20, 2017." [Online]. Available: http://www.solar-frontier.com/eng/news/2017/1220_press.html. [Accessed: 11-Jun-2018].

[2] P. Jackson, R. Wuerz, D. Hariskos, E. Lotter, W. Witte, M. Powalla, Effects of heavy alkali elements in Cu(In,Ga)Se_2 solar cells with efficiencies up to 22.6%, Phys. Status Solidi RRL - Rapid Res. Lett. (2016).

[3] M. Edoff, S. Schleussner, E. Wallin, O. Lundberg, Technological and economical aspects on the influence of reduced Cu(In,Ga)Se2 thickness and Ga grading for co-evaporated Cu(In,Ga)Se2 modules, Thin Solid Films 519, 21 (2011).
[4] K. A. W. Horowitz, M. Woodhouse, Cost and potential of monolithic CIGS photovoltaic modules, Photovolt. Spec. Conf. PVSC, 2015 IEEE 42nd (2015) 1-6.
[5] B. Vermang, J. T. Wätjen, C. Frisk, V. Fjällström, F. Rostvall, M. Edoff, P. Salomé, J. Borme, N. Nicoara, S. Sadewasser, Introduction of Si PERC Rear Contacting Design to Boost Efficiency of Cu(In,Ga)Se Solar Cells, IEEE J. Photovolt. 4, 6 (2014).
[6] Z. Jehl, F. Erfurth, N. Naghavi, L. Lombez, I. Gerard, M. Bouttemy, P. Tran-Van, A. Etcheberry, G. Voorwinden, B. Dimmler, W. Wischmann, M. Powalla, J. F. Guillemoles, D. Lincot, Thinning of CIGS solar cells: Part II: Cell characterizations, Thin Solid Films 519, 21 (2011).
[7] F. Mollica, M. Jubault, F. Donsanti, A. Loubat, M. Bouttemy, A. Etcheberry, N. Naghavi, Light absorption enhancement in ultra-thin Cu(In,Ga)Se2 solar cells by substituting the back-contact with a transparent conducting oxide based reflector, Thin Solid Films 633 (2017) 202–207.
[8] K. Orgassa, H. W. Schock, J. H. Werner, Alternative back contact materials for thin film Cu(In,Ga)Se2 solar cells, Thin Solid Films 431–432 (2003) 387–391.
[9] Z. J. Li-Kao, N. Naghavi, F. Erfurth, J. F. Guillemoles, I. Gérard, A. Etcheberry, J. L. Pelouard, S. Collin, G. Voorwinden, D. Lincot, Towards ultrathin copper indium gallium diselenide solar cells: proof of concept study by chemical etching and gold back contact engineering: CIGSe: chemical etching and gold back contact engineering, Prog. Photovolt. Res. Appl. 20, 5 (2012).
[10] S. Schleussner, T. Kubart, T. Törndahl, M. Edoff, Reactively sputtered ZrN for application as reflecting back contact in Cu(In,Ga)Se2 solar cells, Thin Solid Films 517, 18 (2009).
[11] B. Vermang, J. T. Wätjen, V. Fjällström, F. Rostvall, M. Edoff, R. Gunnarsson, I. Pilch, U. Helmersson, R. Kotipalli, F. Henry, D. Flandre, Highly reflective rear surface passivation design for ultra-thin Cu(In,Ga)Se2 solar cells, Thin Solid Films 582 (2015) 300–303.
[12] J. Goffard, C. Colin, F. Mollica, A. Cattoni, C. Sauvan, P. Lalanne, J. F. Guillemoles, N. Naghavi, S. Collin, Light Trapping in Ultrathin CIGS Solar Cells with Nanostructured Back Mirrors, IEEE J. Photovolt. 7, 5 (2017).
[13] G. Yin, M. W. Knight, M.-C. van Lare, M. M. Solà Garcia, A. Polman, M. Schmid, Optoelectronic Enhancement of Ultrathin $CuIn_{1-x}Ga_xSe_2$ Solar Cells by Nanophotonic Contacts, Adv. Opt. Mater. 5, 5 (2017).
[14] V. E. Ferry, M. A. Verschuuren, M. C. van Lare, R. E. I. Schropp, H. A. Atwater, A. Polman, Optimized Spatial Correlations for Broadband Light Trapping Nanopatterns in High Efficiency Ultrathin Film a-Si:H Solar Cells, Nano Lett. 11, 10 (2011).
[15] W. Yang, J. Becker, S. Liu, Y. S. Kuo, J. J. Li, B. Landini, K. Campman, Y. H. Zhang, Ultra-thin GaAs single-junction solar cells integrated with a reflective back scattering layer, J. Appl. Phys. 115, 20, (2014).
[16] H.-L. Chen, A. Cattoni, N. Vandamme, J. Goffard, A. Lemaitre, A. Delamarre, B. Behaghel, K. Watanabe, M. Sugiyama, J. F. Guillemoles, S. Collin, 200nm-thick GaAs solar cells with a nanostructured silver mirror, Photovolt. Spec. Conf. PVSC, 2016 IEEE 43rd (2016) 3506-3509.
[17] J. Keller, W.-C. Chen, L. Riekehr, T. Kubart, T. Törndahl, M. Edoff, Bifacial $Cu(In,Ga)Se_2$ solar cells using hydrogen-doped In_2O_3 films as a transparent back contact, Prog. Photovolt. Res. Appl. 26, 10 (2018).

[18] H. Simchi, J. Larsen, K. Kim, W. Shafarman, Improved Performance of Ultrathin Cu(InGa)Se2 Solar Cells With a Backwall Superstrate Configuration, IEEE J. Photovolt. 4, 6 (2014).
[19] W. Ohm, W. Riedel, Ü. Aksünger, D. Greiner, C. A. Kaufmann, M. C. Lux-Steiner, S. Gledhill, Bifacial Cu(In,Ga)Se2 solar cells with submicron absorber thickness: back-contact passivation and light management, Photovolt. Spec. Conf. PVSC, 2015 IEEE 42nd (2015) 1-5.
[20] M. Terheggen, H. Heinrich, G. Kostorz, F.-J. Haug, H. Zogg, A. N. Tiwari, Ga2O3 segregation in Cu(In,Ga)Se2/ZnO superstrate solar cells and its impact on their photovoltaic properties, Thin Solid Films 403–404 (2002) 212-215
[21] M. D. Heinemann, F. Ruske, D. Greiner, A. R. Jeong, M. Rusu, B. Rech, R. Schlatmann, C. A. Kaufmann, Advantageous light management in Cu(In,Ga)Se2 superstrate solar cells, Sol. Energy Mater. Sol. Cells 150 (2016) 76-81.
[22] T. Nakada, Microstructural and diffusion properties of CIGS thin film solar cells fabricated using transparent conducting oxide back contacts, Thin Solid Films 480–481 (2005) 419-425.
[23] T. Nakada, Y. Hirabayashi, T. Tokado, D. Ohmori, T. Mise, Novel device structure for Cu(In,Ga)Se2 thin film solar cells using transparent conducting oxide back and front contacts, Sol. Energy 77, 6 (2004).
[24] T. Klinkert, M. Jubault, F. Donsanti, D. Lincot, J.-F. Guillemoles, Ga gradients in Cu(In,Ga)Se_2 : Formation, characterization, and consequences, J. Renew. Sustain. Energy 6, 1 (2014).
[25] T. Bottein, O. Dalstein, M. Putero, A. Cattoni, M. Faustini, M. Abbarchia, D. Grosso, Environment-controlled sol–gel soft-NIL processing for optimized titania, alumina, silica and yttria-zirconia imprinting at sub-micron dimensions, Nanoscale 10, 3 (2018).
[26] O. Dalstein, D. R. Ceratti, C. Boissière, D. Grosso, A. Cattoni, M. Faustini, Nanoimprinted, Submicrometric, MOF-Based 2D Photonic Structures: Toward Easy Selective Vapors Sensing by a Smartphone Camera, Adv. Funct. Mater. 26 (2016) 81-90.

List of figures

Fig. 1 Sketch of an ultrathin CIGS solar cell a) on planar back contacts such as molybdenum, TCO, or reflective multi-layer stack (MLS) and b) on a nanostructured back mirror consisting of a periodically patterned dielectric on top of reflective MLS. c) Three dimensional view of the ultrathin device on a nanostructured back mirror with optimized geometry. CIGS is deposited on top of a square-shaped dielectric nanogrid with a height of 200 nm, a period of 600 nm and hole width of 350 nm.

Fig. 2 Simulated absorption within each layer of 490 nm thick CIGS solar cells under AM1.5G illumination, with back contacts made of a) molybdenum, b) ITO, c) reflective multi-layer stack (MLS) and d) reflective MLS with nanopatterns. Respective experimental EQEs are given in a), b) and c) for comparison.

Fig. 3. a) Reflectance of 600 nm thick molybdenum (grey), 150 nm thick silver (black) and stacks of 30 nm thick (red) and 200 nm thick (blue) ITO on silver before and after annealing in air at 540 °C for 10 minutes (dashed and solid lines, respectively). b) Refractive index n (solid lines) and extinction coefficient k (dashed lines) of a 200 nm thick sputtered ITO layer measured by ellipsometry before (black) and after (red) annealing.

Fig. 4 a) TEM dark field image of ultrathin CIGS layer deposited on ITO back contact with b) corresponding composition profile from average EDX signal, c) TEM dark field image of ultrathin CIGS layer close to the ITO back contact with associated EDX mappings of O, Ga, In, and Se elements.

Fig. 5 Experimental I(V) and External Quantum Efficiency (EQE) curves of 490 nm thick CIGS solar cells on molybdenum (black), ITO (red) and reflective multi-layer stack (blue) back contacts.

Table captions

Table 1. Summary of I(V) parameters for 490 nm thick CIGS solar cells with various back contacts. A two-diode model is used to fit dark I(V) curves (J_{01} and J_{02}: saturation currents for respective ideality factors of 1 and 2, R_{SH}: shunt resistance, R_S: series resistance).

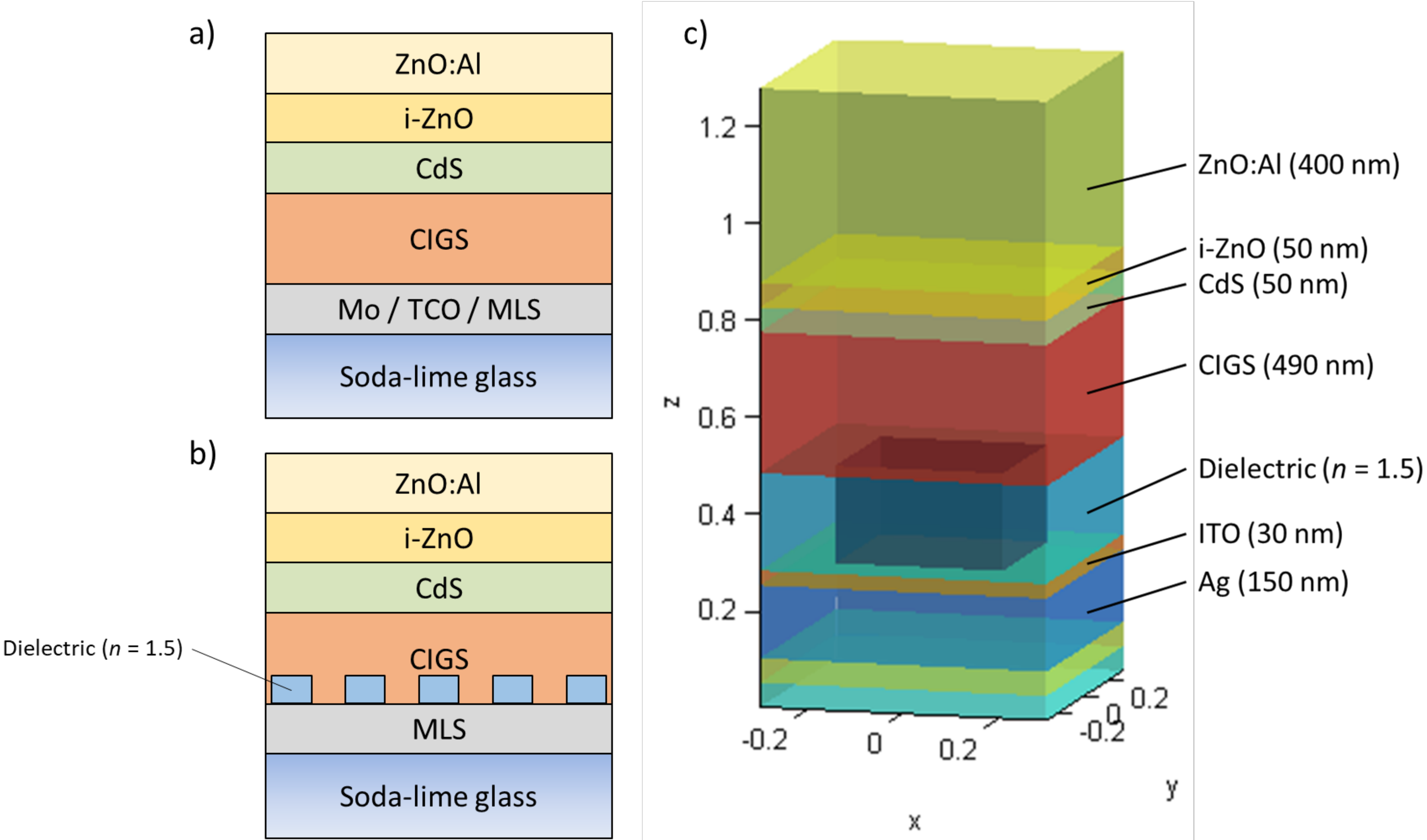

a)
ZnO:Al
i-ZnO
CdS
CIGS
Mo / TCO / MLS
Soda-lime glass
b)
ZnO:Al
i-ZnO
CdS
CIGS
Dielectric (n = 1.5)
MLS
Soda-lime glass
c)
ZnO:Al (400 nm)
i-ZnO (50 nm)
CdS (50 nm)
CIGS (490 nm)
Dielectric (n = 1.5)
ITO (30 nm)
Ag (150 nm)
z
1.2
1
0.8
0.6
0.4
0.2
-0.2
0
0.2
x
y

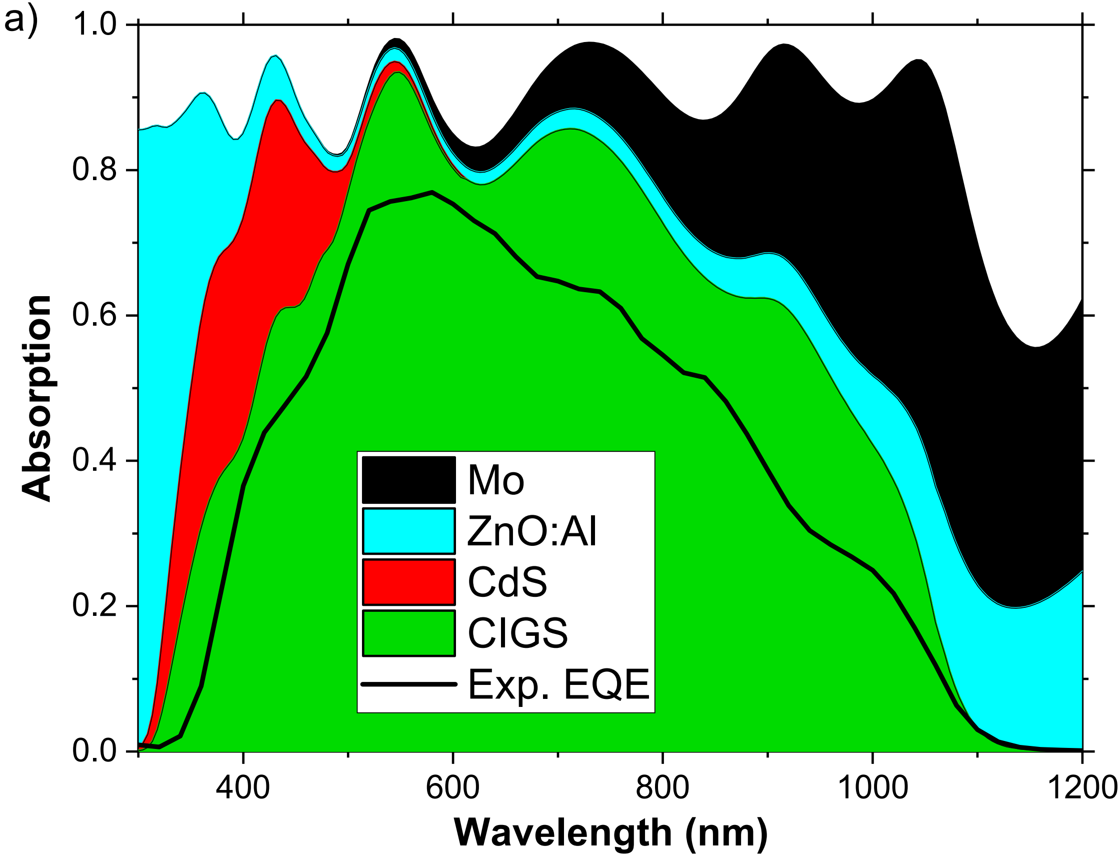

a)
1.0
0.8
0.6
0.4
0.2
0.0
Absorption
400
600
800
1000
1200
Wavelength (nm)
Mo
ZnO:Al
CdS
CIGS
Exp. EQE

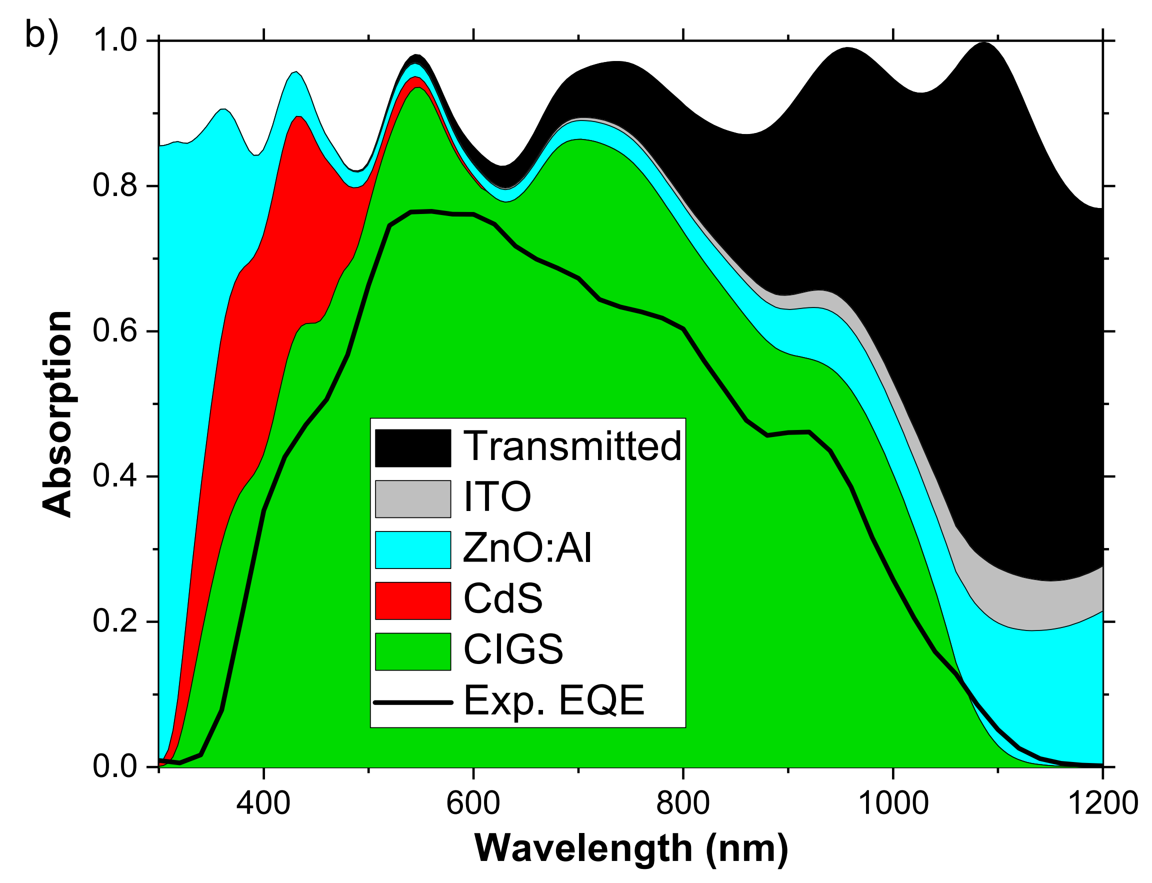

b)
Absorption
Wavelength (nm)
0.0
0.2
0.4
0.6
0.8
1.0
400
600
800
1000
1200
Transmitted
ITO
ZnO:Al
CdS
CIGS
Exp. EQE

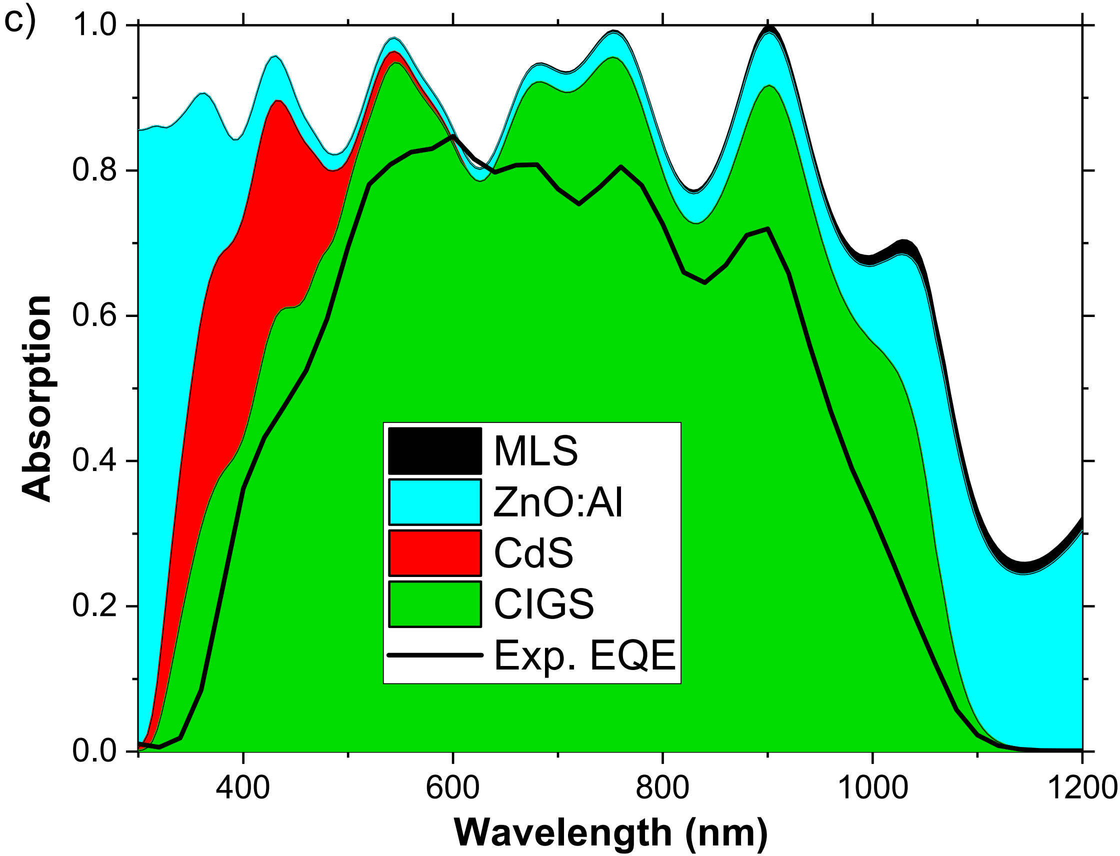
c)
Absorption
Wavelength (nm)
1.0
0.8
0.6
0.4
0.2
0.0
400
600
800
1000
1200
MLS
ZnO:Al
CdS
CIGS
Exp. EQE

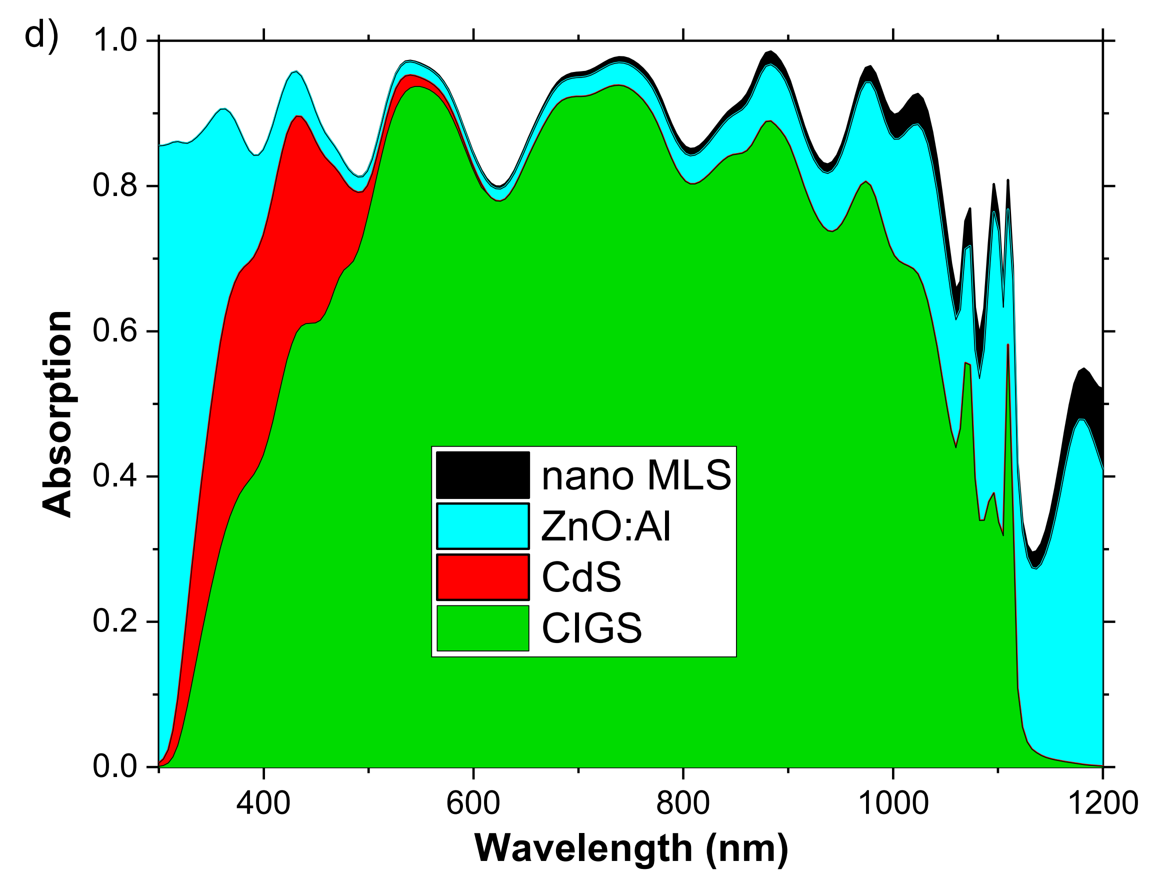
d)
Absorption
Wavelength (nm)
0.0
0.2
0.4
0.6
0.8
1.0
400
600
800
1000
1200
nano MLS
ZnO:Al
CdS
CIGS

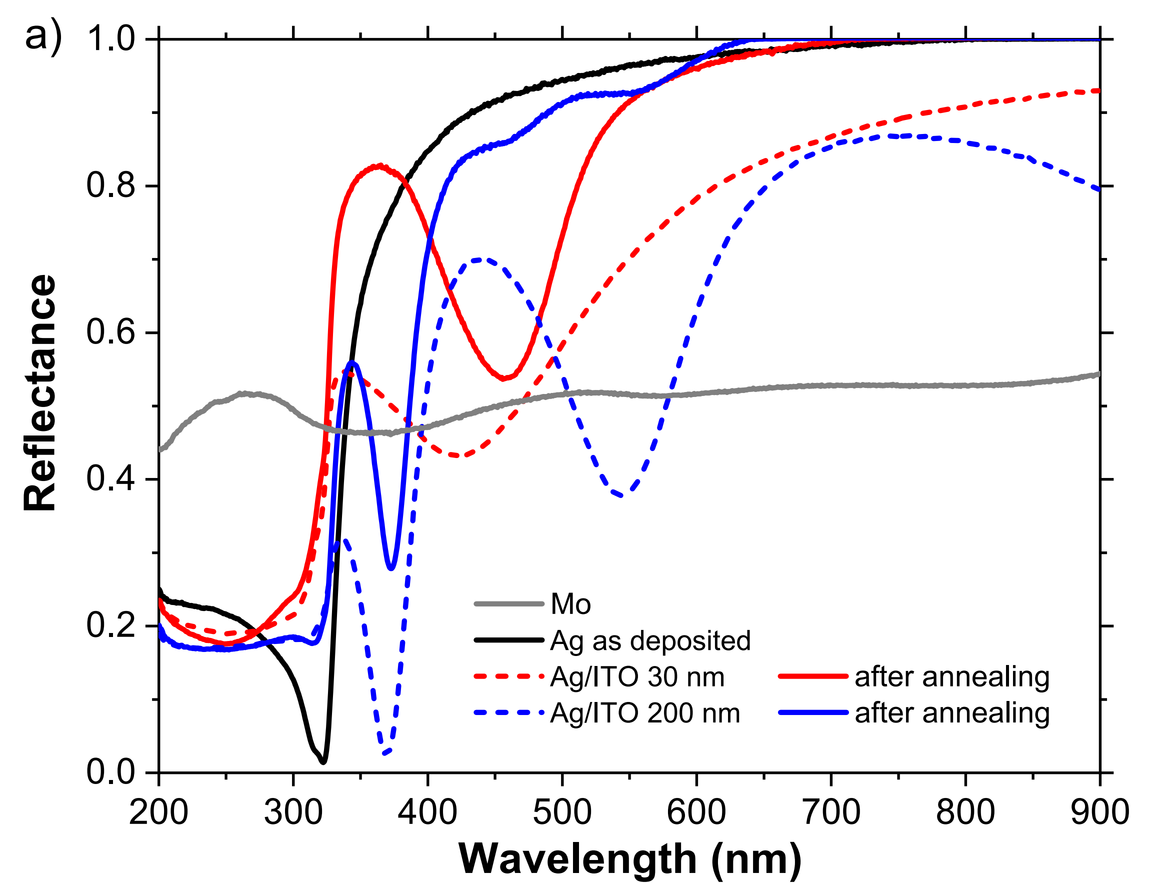

a)
Reflectance
Wavelength (nm)
0.0
0.2
0.4
0.6
0.8
1.0
200
300
400
500
600
700
800
900
Mo
Ag as deposited
Ag/ITO 30 nm
after annealing
Ag/ITO 200 nm
after annealing

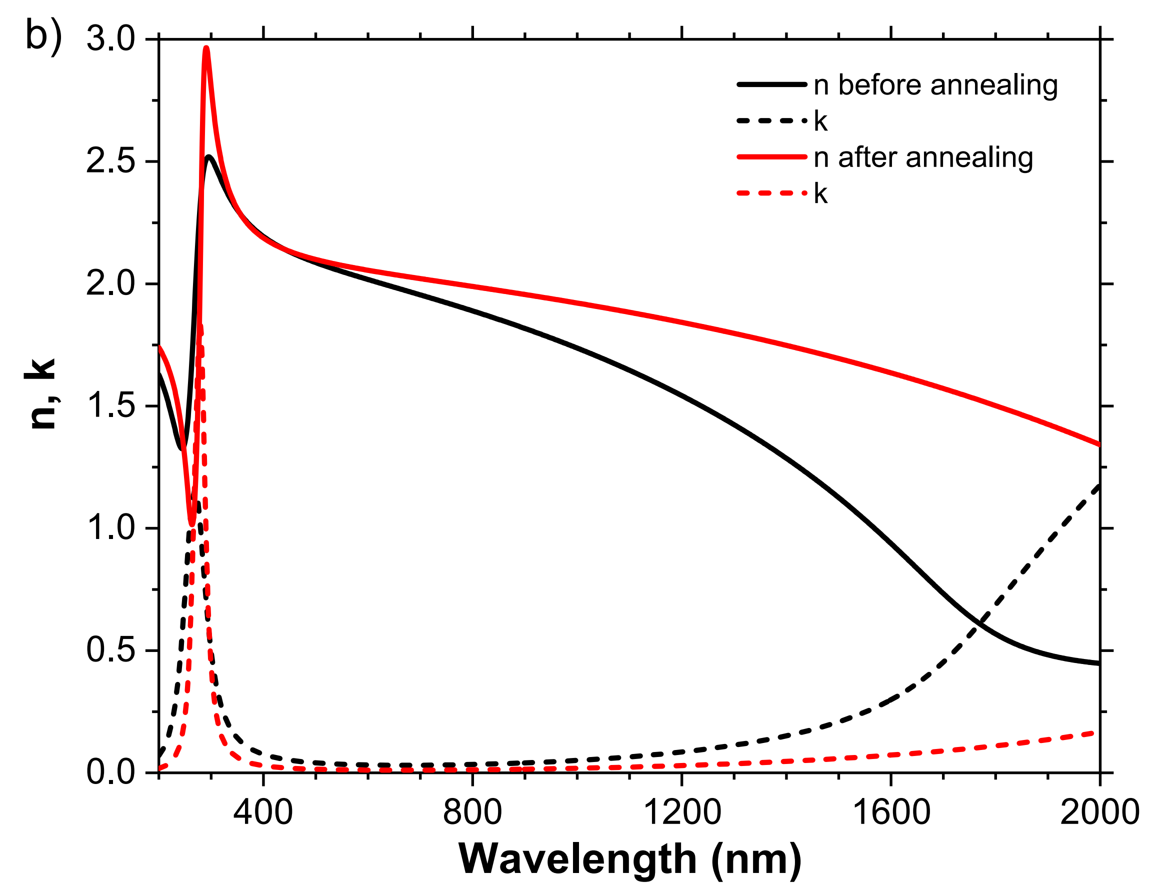
b)
n before annealing
k
n after annealing
k
n, k
3.0
2.5
2.0
1.5
1.0
0.5
0.0
400
800
1200
1600
2000
Wavelength (nm)

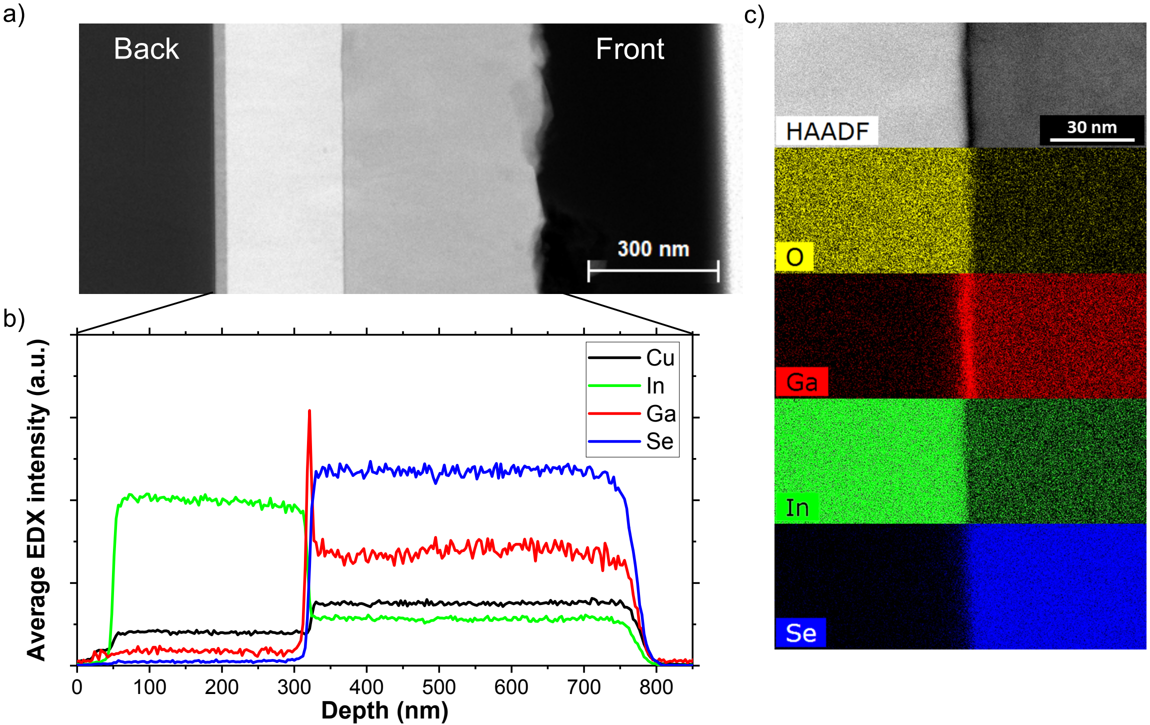
a)
Back
Front
300 nm
b)
Average EDX intensity (a.u.)
Depth (nm)
0
100
200
300
400
500
600
700
800
Cu
In
Ga
Se
c)
HAADF
30 nm
O
Ga
In
Se

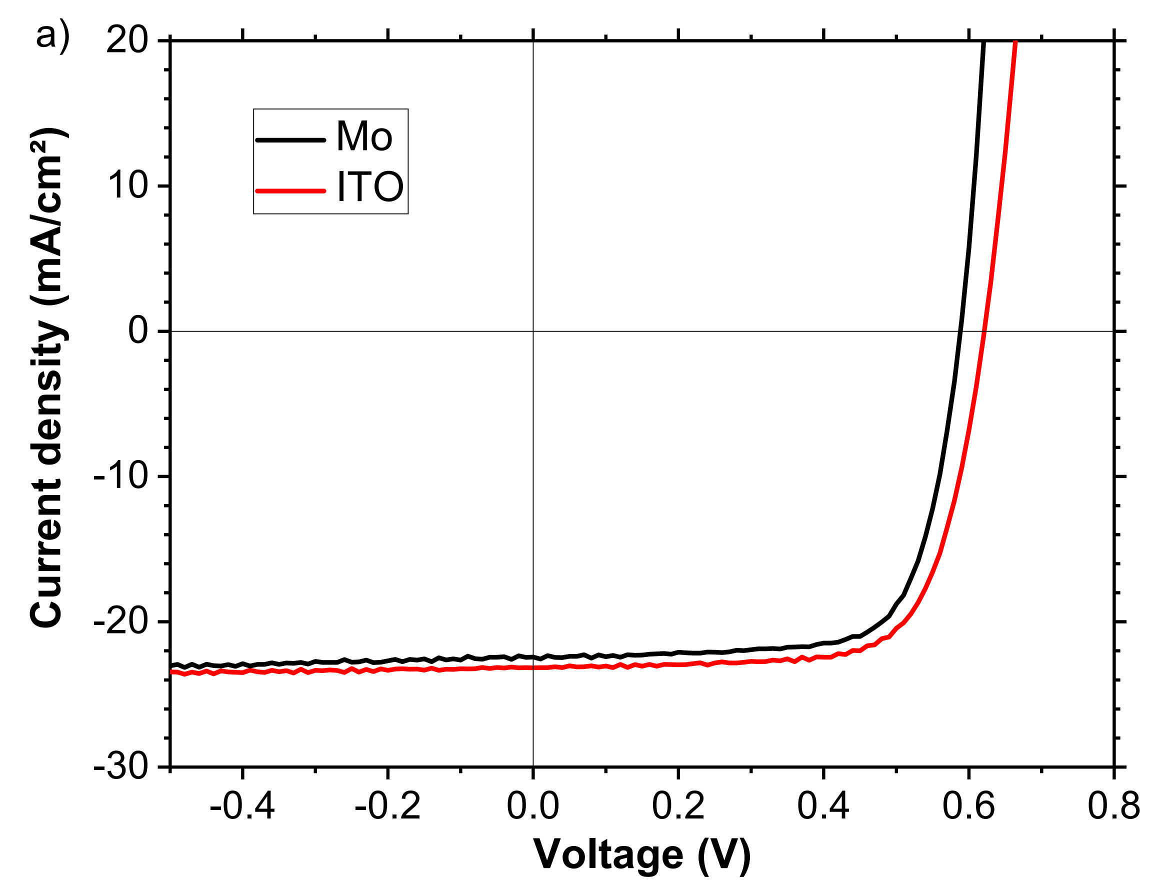
a)
Mo
ITO
Current density (mA/cm²)
Voltage (V)
20
10
0
-10
-20
-30
-0.4
-0.2
0.0
0.2
0.4
0.6
0.8

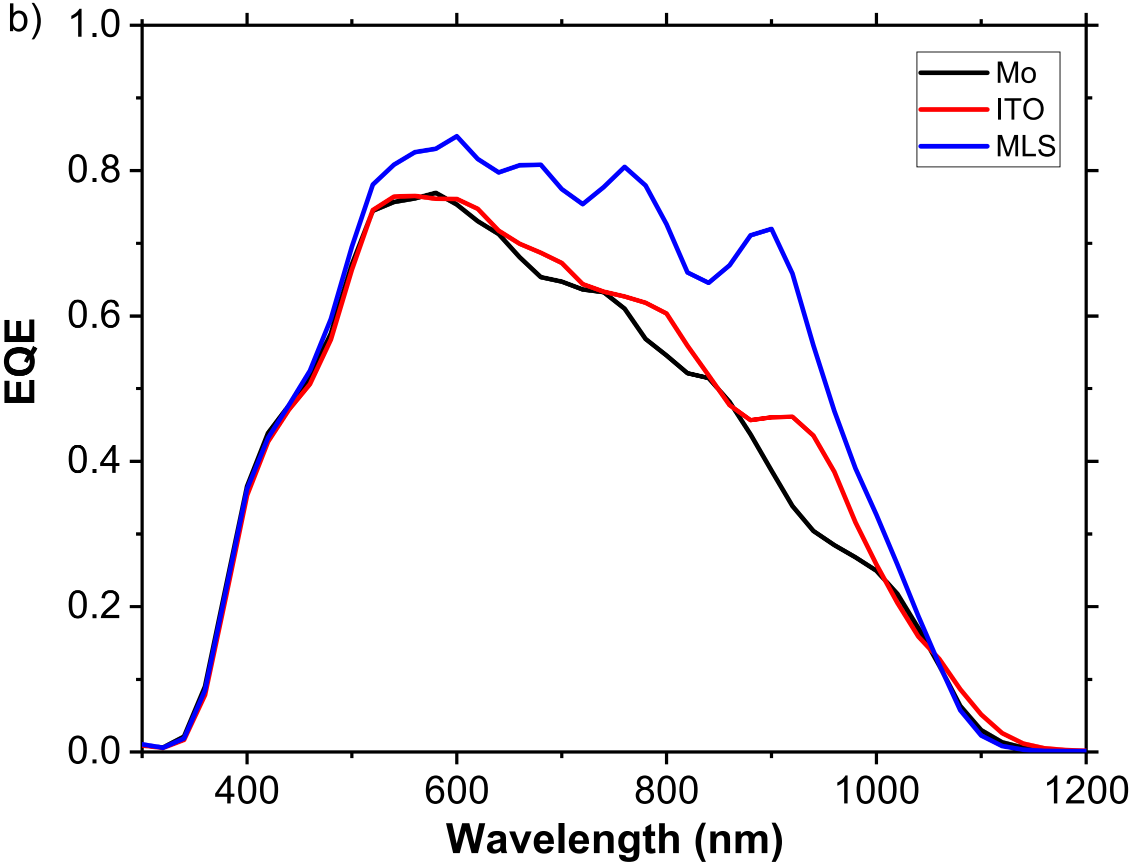
b)
EQE
Wavelength (nm)
Mo
ITO
MLS
0.0
0.2
0.4
0.6
0.8
1.0
400
600
800
1000
1200